Freshwater discharges drive high levels of methylmercury in Arctic marine biota

Amina T. Schartup[a,b,1], Prentiss H. Balcom[b,c], Anne L. Soerensen[a], Kathleen J. Gosnell[c], Ryan S. D. Calder[a,b], Robert P. Mason[c], and Elsie M. Sunderland[a,b]

[a]Department of Environmental Health, Harvard T. H. Chan School of Public Health, Boston, MA 02215; [b]John A. Paulson School of Engineering and Applied Sciences, Harvard University, Cambridge, MA 02138; and [c]Department of Marine Sciences, University of Connecticut, Groton, CT 06340

Edited by Vincent L. St. Louis, University of Alberta, Edmonton, AB, Canada, and accepted by the Editorial Board August 4, 2015 (received for review March 19, 2015)

Elevated levels of neurotoxic methylmercury in Arctic food-webs pose health risks for indigenous populations that consume large quantities of marine mammals and fish. Estuaries provide critical hunting and fishing territory for these populations, and, until recently, benthic sediment was thought to be the main methylmercury source for coastal fish. New hydroelectric developments are being proposed in many northern ecosystems, and the ecological impacts of this industry relative to accelerating climate changes are poorly characterized. Here we evaluate the competing impacts of climate-driven changes in northern ecosystems and reservoir flooding on methylmercury production and bioaccumulation through a case study of a stratified sub-Arctic estuarine fjord in Labrador, Canada. Methylmercury bioaccumulation in zooplankton is higher than in midlatitude ecosystems. Direct measurements and modeling show that currently the largest methylmercury source is production in oxic surface seawater. Water-column methylation is highest in stratified surface waters near the river mouth because of the stimulating effects of terrestrial organic matter on methylating microbes. We attribute enhanced biomagnification in plankton to a thin layer of marine snow widely observed in stratified systems that concentrates microbial methylation and multiple trophic levels of zooplankton in a vertically restricted zone. Large freshwater inputs and the extensive Arctic Ocean continental shelf mean these processes are likely widespread and will be enhanced by future increases in water-column stratification, exacerbating high biological methylmercury concentrations. Soil flooding experiments indicate that near-term changes expected from reservoir creation will increase methylmercury inputs to the estuary by 25–200%, overwhelming climate-driven changes over the next decade.

mercury | plankton | estuary | biomagnification | hydroelectric reservoir

Methylmercury (MeHg) is a potent neurotoxin that biomagnifies in marine food-webs (1). Indigenous populations in the Arctic are exposed to elevated levels of MeHg through their traditional diet of fish and marine mammals (2). Elevated biological MeHg concentrations are widely reported across the Arctic and sub-Arctic, a region lacking concentrated anthropogenic Hg sources (3). Anthropogenic Hg is distributed globally in the atmosphere and oceans and is transported to the Arctic where it may be converted to biologically available MeHg by methylating microbes. Naturally present inorganic Hg also can pose a threat to Arctic biota when environmental conditions are perturbed in a manner that stimulates the activity of methylating microbes, one such example being reservoir creation (4). Here, we investigate potential drivers of MeHg production and uptake at the base of the marine food-web in a sub-Arctic estuarine fjord, Lake Melville in Labrador, Canada. We use this information to understand better how changes in high-latitude marine ecosystems driven by climate and industry are likely to affect biological MeHg burdens.

MeHg production in inland ecosystems and estuaries has been attributed mainly to benthic sediment where geochemical conditions that facilitate methylation by anaerobic bacteria are commonly found (5, 6). In open-ocean seawater, strong associations between methylated Hg concentrations and nutrients, apparent oxygen utilization (AOU), and organic carbon remineralization rates (OCRR) are observed across major basins (7–10). These associations reflect subsurface water-column production of MeHg and coincide with peaks in heterotrophic bacterial activity (7–10). In the Arctic Ocean water column, peak methylation rates and ambient MeHg concentrations occur at much shallower depths than observed at midlatitudes but also are correlated with AOU (11, 12). No comparable measurements for high-latitude estuaries are available.

Lake Melville is a large (length, 180 km; surface area, 3,000 km^2), deep (maximum depth, 256 m; mean depth, 83.5 m) semienclosed estuarine fjord (*SI Appendix*, Fig. S1). A dominant feature of this system is a low-salinity surface layer at a depth of 2–15 m that remains intact year round at the estuarine surface (13). Stratification is most pronounced in the estuary near the mouth of the main freshwater tributary and gradually breaks down in the outer marine reaches approaching the Labrador Sea (Fig. 1). During the fall and winter months cold outer Labrador Sea water replaces the saline deep waters without altering the halocline structure (13). The system is ice covered during the winter months and thaws in the spring. More than 60% of the freshwater inputs to Lake Melville are from the Churchill River, where development of a new reservoir for hydroelectric power is underway (*SI Appendix*, Fig. S1).

Flooding associated with reservoirs causes a long-term increase in MeHg production resulting from decomposing organic matter and changes in the geochemical environment that stimulate methylating bacteria (4, 14, 15). With increasing demand for renewable energy,

Significance

Estuaries are the predominant hunting and fishing territory for northern indigenous populations whose way of life is threatened by both climate change and industrial development. Direct measurements and modeling conducted as part of this study show enhanced production of methylmercury, a potent neurotoxin, and uptake by plankton in stratified oxic seawater. Enhanced climate-driven stratification of ocean margin areas with sea-ice melt will likely elevate biological methylmercury concentrations in the Arctic. Elevated biological methylmercury levels will be exacerbated by hydroelectric development planned throughout many northern regions. Our experimental measurements indicate that, over the next decade, regional increases in methylmercury concentrations resulting from flooding associated with hydroelectric development will be greater than those expected from climate change.

Author contributions: A.T.S. and E.M.S. designed research; A.L.S. and R.S.D.C. helped with the modeling; A.T.S. performed research; P.H.B. and R.P.M. contributed analytic tools; A.T.S., P.H.B., K.J.G., and E.M.S. analyzed data; and A.T.S. and E.M.S. wrote the paper.

The authors declare no conflict of interest.

This article is a PNAS Direct Submission. V.L.S.L. is a guest editor invited by the Editorial Board.

[1]To whom correspondence should be addressed. Email: schartup@hsph.harvard.edu.

This article contains supporting information online at www.pnas.org/lookup/suppl/doi:10.1073/pnas.1505541112/-/DCSupplemental.

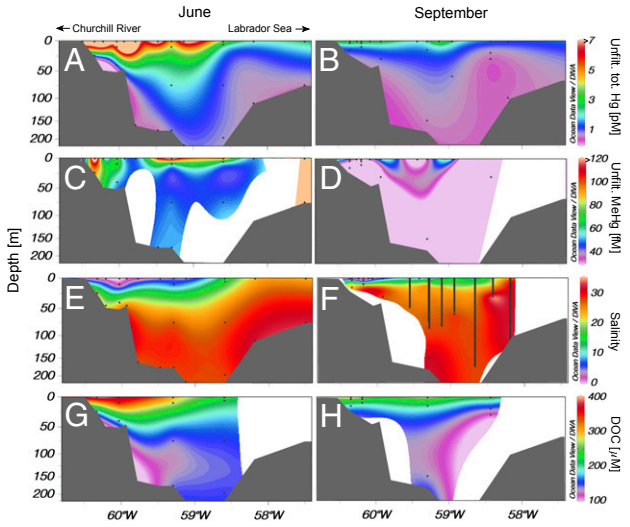

Fig. 1. Cross-sectional view of total Hg and MeHg concentrations in unfiltered seawater in Lake Melville extending from the freshwater inputs on the left (Churchill River) to outer marine regions (Groswater Bay) on the right that extend into the Labrador Sea. (*A* and *B*) Unfiltered total Hg. (*C* and *D*) Unfiltered total MeHg. (*E* and *F*) Salinity. (*G* and *H*) Dissolved organic carbon. Samples were collected between August 31 and September 8, 2012 and June 11–19, 2013. Black symbols represent sampling points. Bars in *F* represent a measurement frequency of 0.1–0.5 m.

new hydroelectric developments are being proposed in many northern ecosystems, and the ecological impacts of this industry are poorly characterized. Research in the Experimental Lakes Area of Canada showed a 40-fold increase in aqueous MeHg concentrations following large-scale flooding and increased biological concentrations that persisted for more than a decade (4, 14, 15). Here we discuss the magnitude of potential changes driven by hydroelectric development compared with future climate-driven effects.

The main objective of this study is to evaluate the environmental drivers of MeHg production and bioaccumulation in high-latitude ocean margin regions. We hypothesized that terrestrial discharges would be a large source of Hg and MeHg in the marine waters of this fjord and thus that reservoir flooding would impact biological MeHg concentrations substantially. We tested this hypothesis through an evaluation of major MeHg sources and biological uptake throughout the estuary. Seawater, benthic sediment, and zooplankton were obtained along a salinity gradient from freshwater regions to the outer Labrador Sea from August 31 to September 8, 2012 (27 stations) and from June 11–19, 2013 (18 stations). Using enriched mercury isotope spikes, we directly measured the production (methylation) and decomposition (biotic/dark demethylation) of MeHg in the marine water column and benthic sediment at multiple stations to assess the importance of in situ production compared with external inputs.

MeHg Production in Estuarine Seawater

Vertical profiles of Hg, MeHg, and dissolved organic carbon (DOC) are strongly influenced by the stable year-round halocline of Lake Melville. Fig. 1 shows total Hg and DOC in the Lake Melville water column are enriched in the low-salinity surface layer compared with the saline deep waters supplied by the Labrador Sea. This pattern is consistent with inputs from rivers being the major source of total Hg and DOC to Lake Melville and is reinforced by strong correlations between aqueous total Hg concentrations, salinity, and DOC (*SI Appendix*, Table S1). Total Hg concentrations are increased by spring snowmelt when concentrations in rivers and the surface waters of the estuary (Goose Bay and Lake Melville) are significantly ($P < 0.01$, t test) higher than in the fall (Table 1 and *SI Appendix*, Table S2).

We calculated potential inorganic Hg methylation rates at multiple stations of up to 0.4%·d^{-1} in June 2013 from single-time-point measurements of seawater incubated for 24 h (Fig. 2*A*). Methylation rates were below detection at the river sampling sites (*SI Appendix*, Table S3) and were highest in the estuarine regions close to the river mouth (Fig. 2*A*). Water-column dark (biotic) demethylation rates were below 2%·d^{-1}, which is on the low end of previous observations (*SI Appendix*, Table S3). Measureable methylation in combination with low demethylation in this system results in the net accumulation of MeHg in these surface waters.

The MeHg distribution in Lake Melville reflects the combined influences of direct inputs from rivers and methylation in surface waters (Fig. 1). MeHg is significantly correlated with salinity in September ($P < 0.01$), but not in June, as is consistent with the growing importance of in situ production in the spring (*SI Appendix*, Fig. S2 and Table S3). Ambient MeHg concentrations in the upper few meters of the estuarine water column are enriched from riverine inputs rather than water-column methylation relative to deeper waters within the stratified low-salinity surface layer. Concentrations of MeHg are extremely low throughout the cold, saline deep waters of Lake Melville.

Table 1. Summary of measured mercury species concentrations (mean ± standard deviation) across the Lake Melville region in September 2012 and June 2013

	Tributaries		Goose Bay		Lake Melville		Groswater Bay	
	September 2012	June 2013	September 2012	June 2013	September 2012	June 2013	September 2012	June 2013
Unfiltered water								
Total Hg, pM	3.6 ± 0.1	11.4 ± 3.0	2.5 ± 1.0	7.0 ± 5.2	1.9 ± 1.5*	4.0 ± 3.2*	1.0 ± 0.6	1.5 ± 1.0
MeHg, fM	68 ± 8	40 ± 15	48 ± 12	84 ± 40	40 ± 19	91 ± 52	bd	116 ± 58
Hg^0, fM	22, 245	141 ± 118	40 ± 6	69†	61 ± 29	97 ± 18	n/d	66 ± 2
Suspended solids partition coefficient, log K_P								
Total Hg	4.5 ± 0.3	n/d	5.0 ± 0.3	4.8 ± 0.7	4.6 ± 0.5	4.0 ± 0.5	n/d	n/d
MeHg	4.4†	n/d	3.9 ± 0.5	4.4 ± 0.7	4.5†	3.6 ± 0.7	n/d	n/d
Sediment, mol·g^{-1}								
Total Hg	55 ± 43	8, 23,126	70 ± 28	83 ± 10	173 ± 67	167 ± 100	117†	73†
MeHg	0.3 ± 0.4	2.2 ± 2.2	0.7 ± 0.5	1.9 ± 0.9	0.3 ± 0.2	1.6 ± 1.2	0.6†	4.0 ± 0.03

bd, below detection; n/d, no data.

*Two Lake Melville sites with strong riverine influence were excluded. Total Hg measured close to the North West (*SI Appendix*, Fig. S1, Station 1) and Kenamu (*SI Appendix*, Fig. S1, Station 2) Rivers was 13.9 and 28.7, respectively.

†No standard deviation is listed because only one sample is available.

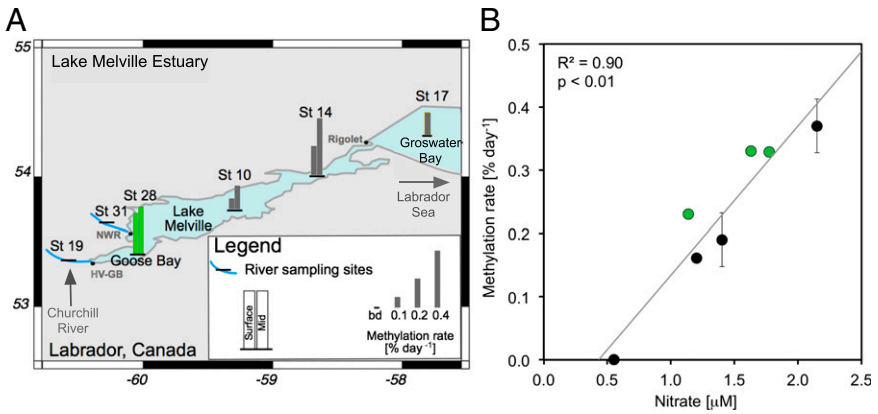

Fig. 2. Measured methylation rates and MeHg concentrations in Lake Melville. (*A*) Distribution of surface and middepth methylation rates in Lake Melville. Sample collection stations are noted near the symbols. (*B*) Linear relationship between water-column methylation rates in Lake Melville (black symbols) and Goose Bay (green symbols) and nitrate.

We found a strong correlation between water-column methylation rates and nitrate in the low-salinity surface layer of the estuary (Fig. 2*B*). Stepwise regression analysis on a suite of parameters shows that nitrate alone explains 90% of the variability in measured methylation rates ($P < 0.01$). We postulate that this finding reflects the association between the degradation of organic matter in surface waters and MeHg production proposed by others (7–10).

Prior work in the upper ocean suggests that production of methylated Hg species is linked to heterotrophic bacterial activity responsible for the turnover of organic carbon in the marine water column, as reflected by changes in nitrate, phosphate, AOU, and OCRR (7–11). Lake Melville is oligotrophic, and nitrate concentrations in inflowing tributaries are low (<3 μM). Nitrate is depleted by algal growth (1–2 μM) at the surface and is replenished below (3–6 μM) by the release of nutrients during the degradation of organic matter (*SI Appendix*, Fig. S3). We find methylation rates are higher approaching the thermocline (6–10 m) than in measurements made immediately below the surface (1 m). This observation may reflect greater heterotrophic bacterial activity with depth, as indicated by the increase in nitrate concentrations (*SI Appendix*, Fig. S3). We find extremely low concentrations of MeHg in the deep waters of Lake Melville that have high dissolved oxygen and are replenished by seawater from the outer Labrador Sea every 4–5 mo (13). Nutrient concentrations in these waters are decoupled from surface biological processes by strong vertical stratification.

We attribute the large increase in ambient MeHg concentrations between the rivers and the surface water of the estuary to active water-column methylation (Table 1 and *SI Appendix*, Table S2). We hypothesize that the activity of methylating bacteria is stimulated by redox microniches formed by the aggregation and enhanced degradation of terrestrial DOC in saline waters (7, 16). Visual inspection of estuarine seawater samples revealed high concentrations of flocculated organic material, not present in the river water (*SI Appendix*, Fig. S4), that has been shown to support methylation under laboratory conditions (17). Dissolved organic material in the water column aggregates during the transition from fresh to saline conditions because of the change in ionic strength and the increase in cation concentrations in estuarine water (18). Organic aggregates formed through flocculation in estuaries tend to be enriched in metals and nutrients (cations) and support high microbial diversity (19). Estuarine bacteria degrade terrigenous DOC much faster (up to a fourfold increase at a salinity of four) than do microbes in terrestrial ecosystems (20), explaining the distinct increase in methylation in saline waters.

Stratification Enhances MeHg Bioaccumulation in Plankton

Across marine ecosystems, the majority of MeHg bioaccumulation (10^3–10^5) occurs between seawater and plankton (21, 22). Fig. 3*A* shows a sharp increase in MeHg concentrations between phytoplankton and 200- to 500-μm zooplankton (*SI Appendix*, Table S4). Highest MeHg concentrations and bioaccumulation factors (BAF; plankton MeHg divided by water column MeHg) are observed in the estuarine regions with stable year-round stratification near the river mouth (Goose Bay), and the lowest are observed in the better-mixed outer marine areas (Groswater Bay) (Fig. 3). In the estuary, the fraction of total Hg as MeHg (%MeHg) in different size fractions of plankton increases from <10% in the seston (5–200 μm) to ~80% in the 500- to 1,000-μm size fractions (Fig. 3*A*). Similar increases are not observed in Groswater Bay approaching the Labrador Sea.

We postulate that enhanced bioaccumulation in the stratified regions of the estuary compared with the outer water column reflects a vertically concentrated zone of methylation and biological activity (bacterial activity, phytoplankton, and grazers). Biological hotspots of vertically restricted (on a scale of centimeters to meters) but horizontally dispersed thin layers of marine plankton are common in stratified ecosystems and typically persist from hours to weeks (23, 24). Stratification of the water column facilitates the formation of thin layers of organic material by providing a density surface where settling marine snow reaches neutral buoyancy and can form a mucus-rich mat of aggregated phytoplankton during the spring bloom (25, 26). Stratification also acts as a barrier to turbulent mixing propagated from tidally mixed deep layers (27). Thin layers can collect smaller settling detritus and commonly contain the majority (50–75%) of the phytoplankton biomass in the water column (24). In oligotrophic systems where food for grazing zooplankton is limited and a large proportion of the algal biomass is present in thin layers, herbivorous and predatory zooplankton also are concentrated in this layer (28).

Enhanced microbial activity and organic matter degradation in such a thin layer would explain elevated MeHg production and zooplankton concentrations in the stratified regions of the Lake Melville estuary where BAFs also peak (Fig. 3). Zooplankton communities in this region are dominated by copepods that migrate vertically, such as *Calanus* spp. (29). The concentration of copepod biomass in the thin layer of a stratified fjord compared with outer marine waters has been demonstrated for other Arctic ecosystems (30). Colocation of zooplankton grazers and predators in this vertically restricted zone would enhance trophic structure (lengthen the food chain) and MeHg biomagnification, explaining higher BAFs and %MeHg in the stratified portions of

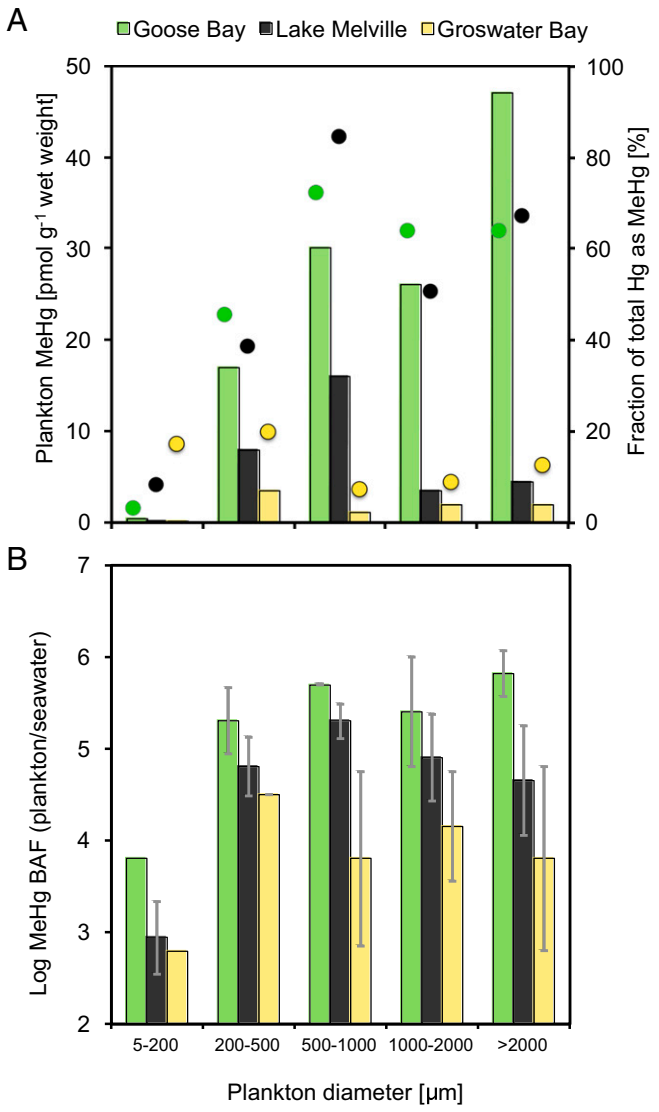

Fig. 3. MeHg in plankton collected in June 2013. (*A*) MeHg concentrations measured in five size classes of plankton across the main sampling regions. The fraction of plankton total Hg as MeHg is represented by circles. Sampling regions are denoted by black (Lake Melville), green (Goose Bay), and yellow (Groswater Bay) bars. (*B*) MeHg BAFs calculated for each size fraction of plankton across the sampling regions (plankton MeHg divided by seawater concentrations). Phytoplankton fall within the 5- to 200-μm size class, and zooplankton comprise the larger fractions.

Lake Melville. Many Arctic copepods are known to be opportunistic feeders that can switch between herbivory and carnivory depending on food availability (31). Thus, vertical migration of copepods, lower seawater MeHg concentrations and production, and more dispersed food sources in the outer Labrador Sea provide a plausible explanation for the lower MeHg concentrations, BAFs, and %MeHg observed in zooplankton from this region.

Riverine Inputs and Water Column Methylation Are Major Sources of MeHg

We constructed an annual mass budget for Hg and MeHg in Lake Melville (Fig. 4) based on field measurements and the modeling framework by Sunderland et al. (32), as described in detail in *SI Appendix*, Tables S5–S8. Rivers are the dominant net source of total Hg inputs [660 mol.annum^{-1} (mol·a^{-1})] followed by direct atmospheric deposition (51 mol·a^{-1}). Tidal inflow is a large gross source of Hg to the estuary (703 mol·a^{-1}), but outflow results in a net loss to the Labrador Sea. Advective inflow of Hg through tidal exchange is confined mainly to the saline deep waters of the estuary because of strong stratification, whereas most biological activity and methylation occur in the upper 15 m of the water column (Fig. 1).

Multiple lines of evidence support the production of MeHg in oxic estuarine surface waters. These include significant increases in methylation potential moving from the rivers into the estuary, net export of MeHg to the Labrador Sea, no evidence for net production in benthic sediment, and insufficient inputs from rivers to explain observed concentrations. Closing the MeHg budget for this system based on riverine MeHg discharges would require inputs three standard deviations beyond our best estimate based on seasonal measurements (*SI Appendix*, Tables S2 and S5), a scenario we find implausible.

To construct a lower-bound estimate of water-column methylation, we apply the mean of measured rates from all regions (*SI Appendix*, Table S1) to the months when methylation is likely occurring (June, July, and August) and assume net production is zero for all other periods. Our resulting estimate of water-column MeHg production (9 mol·a^{-1}) makes it the largest net source in Lake Melville, followed by rivers (5 mol·a^{-1}). MeHg production in oxic surface seawater presently is the major source for the upper stratified water column where biological productivity is concentrated, but this source is expected to change with future alterations of the watershed.

Impacts of Hydroelectric Flooding

We measured MeHg production associated with flooding of soils from the main freshwater tributary of Lake Melville (Churchill River) (Fig. 5). Soil cores were obtained from both inland dry soils in the planned reservoir region and the river shore where occasional flooding already occurs. We removed the litter layer and surface vegetation before saturation with Churchill River water.

We observed a large (14-fold) increase in MeHg concentrations in water overlying inland cores that continued to increase over the 5-d duration of the experiment. A smaller peak in MeHg

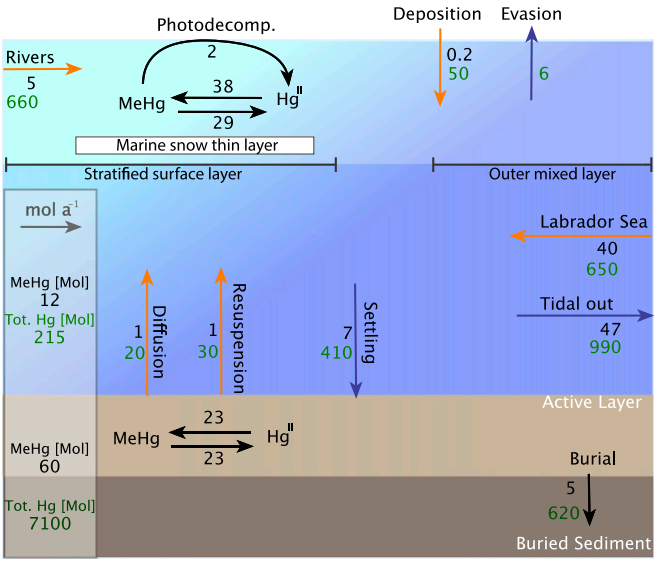

Fig. 4. Empirically constrained annual mass budget for total Hg and MeHg in Lake Melville. Mass flow rates are shown as mol Hg·a^{-1}, and reservoirs are given in moles. Orange arrows represent the input from external sources of MeHg and total Hg to the water column, blue arrows represent losses, and black arrows represent internal fluxes.

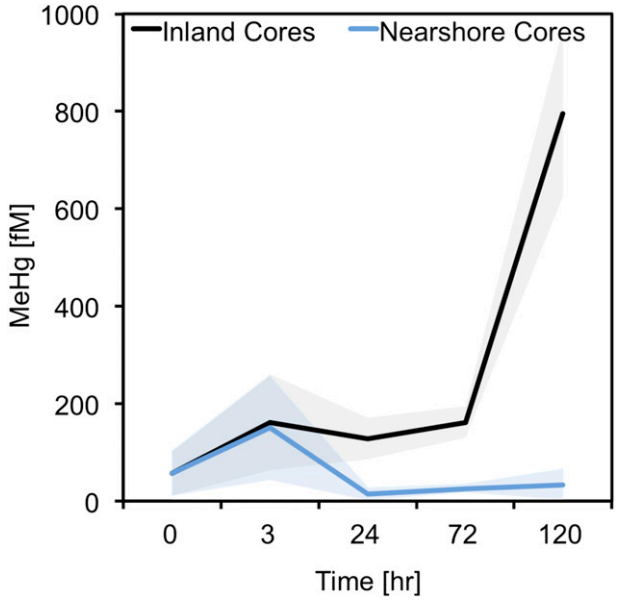

Fig. 5. Temporal changes in the MeHg concentration in water overlying experimentally flooded soils in the Lake Melville watershed (*SI Appendix*, Fig. S1). Results are from six cores from the planned reservoir area. Three were collected near the Churchill River and three from the inland regions that will be flooded.

concentrations, without subsequent increase, was observed after 3 h in cores collected near the river shore (Fig. 5). Virtually all the planned flooded region (41 km^2) will be inland soils with an intact litter layer, in some cases also covered by vegetation and trees (33).

Based on enrichment of MeHg in overlying waters, we calculate a diffusive flux between 120 and 170 $pmol{\cdot}m^{-2}{\cdot}d^{-1}$ across the inland soil cores from the region that will be flooded. This flux is much lower than the peak range of 600–8,000 $pmol{\cdot}m^{-2}{\cdot}d^{-1}$ measured by Hall et al. (4) in the Experimental Lakes Area of Canada. Our measurements represent a lower bound for the increase expected from actual flooding in the Lake Melville region because we removed the litter layer and all vegetation from the surface of the cores, advective fluxes of MeHg are not considered, and MeHg concentrations were still increasing at the end of the 5-d experimental period (Fig. 5). Prior work suggests advective fluxes of MeHg are generally 5–10 times higher than diffusive fluxes (34). Extrapolating the diffusive flux to the planned reservoir regions for Muskrat Falls (41 km^2) (*SI Appendix*, Fig. S1) results in ∼2–3 mol $MeHg{\cdot}a^{-1}$ added to the reservoir and 6–8 mol $MeHg{\cdot}a^{-1}$ for the total development region (126 km^2) that includes an additional reservoir further upstream (Gull Island).

Recent work by Jonsson et al. (35) shows that MeHg bound to terrestrial organic matter is resistant to degradation and readily bioaccumulates. Based on these findings, we assume that approximately half of the diffusive MeHg pulse from the flooded reservoir will enter the Churchill River and be transported into Lake Melville. The resulting lower-bound estimate for changes in MeHg inputs from the Churchill River to Lake Melville is an increase of 25–200%. Plans are in place for clearing most trees but none of the litter layer or other vegetation from the flooded area. We thus postulate that the actual pulse of MeHg to the Lake Melville ecosystem will be much greater, making rivers the dominant MeHg source in the future.

Climate-Driven Changes and Arctic-Wide Implications

Increasing freshwater discharges and ongoing sea-ice melt is expected to increase the stratification of many Arctic marine regions in the future (36). Prior studies in the Canadian Archipelago and Arctic Ocean noted elevated MeHg concentrations in stratified surface waters affected by ice melt (11, 12). Here we suggest that MeHg production and bioaccumulation are enhanced by salinity-driven density gradients in marine waters because of the potential for bacterial activity, associated water-column MeHg production, phytoplankton, and zooplankton grazing to become concentrated in vertically restricted zones. Salinity-driven stratification and water-column methylation fueled by terrestrial DOC sources thus enhance planktonic MeHg exposures and lengthen food-chains, leading to higher biomagnification. Increasing stratification of Arctic marine ecosystems already has been documented, suggesting that these indirect impacts on bioaccumulation are likely widespread and may explain high biological MeHg concentrations in many regions.

Methods

Detailed analytical methods are provided in the *SI Appendix* and are summarized here. We collected water samples 1 m below the water surface at 27 stations in 2012 and 18 stations in 2013 (*SI Appendix*, Fig. S1). We used acid-washed, Teflon-lined General Oceanics GO-FLO sampling bottles and Teflon-coated messengers deployed on a hydrowire (Aracom line, Yale Cordage) following trace-metal-clean protocols (37). We collected at least one additional middepth sample for stations with depths greater than 50 m.

We collected particulate material between 5–200 μm as a proxy for microplankton. Seawater (250–1,500 mL) from surface GO-FLO casts was passed through a 200-μm mesh to remove larger organisms, and particulate material was collected onto 5- to 10-μm acid-cleaned polycarbonate filters (Maine Manufacturing, Fisher Scientific) that were frozen immediately. We collected zooplankton in four size fractions (200–500 μm, 500–1,000 μm, 1,000–2,000 μm, and >2,000 μm) from eight stations (*SI Appendix*, Fig. S1) with a 200-μm trace-metal-clean opening/closing net (Sea Gear Corp.) towed on the hydrowire. Zooplankton from the clean cod end were separated into size fractions using acid-rinsed polycarbonate membrane filters and were frozen immediately.

We incubated sediment from two stations and water from seven stations spiked with isotopically labeled inorganic $^{200}Hg^{II}$ (96.41% purity) and $Me^{199}Hg$. Enriched $Me^{199}Hg$ was prepared from ^{199}Hg (91.95% purity) obtained from Oak Ridge National Laboratory (38, 39). Analytical methods for sediment were as described in Schartup et al. (40). We spiked water samples stored in 250-mL acid-cleaned glass IChem bottles (Fisher Scientific) with $^{200}Hg^{II}$ (∼95 pmol) and $Me^{199}Hg$ (∼0.06 pmol). The magnitudes of isotopic spikes were chosen to follow Lehnherr et al. (11). Spiked natural and deionized waters were incubated for 24 h in the dark at 4 °C, followed by acidification with trace-metal-grade HCl (0.5%, Fisher Scientific).

We simulated the effects of hydroelectric flooding in six cores obtained from two locations in 2013 within the planned flooding region for the Lower Churchill River reservoir (Muskrat Falls) (Fig. 1). Three cores were obtained from a wooded region, and three cores were obtained from an area next to the Churchill River where periodic flooding occurs and that was free from surface vegetation. Each core was submerged in water from the Lower Churchill River in benthic flux chambers as described elsewhere (*SI Appendix*, Fig. S6) (41). Dissolved oxygen was monitored throughout the experiment, and the water was replaced approximately every 24 h to maintain oxic conditions. We measured MeHg, DOC, and nutrients (*SI Appendix*, Fig. S7) in filtered overlying water over 5 d. At the end of the experiment the cores were sectioned in 2-cm increments and frozen. Subsamples of Churchill River water used for these incubations and surface soils from the same locations as cores were analyzed for Hg and MeHg to establish baseline concentrations.

Analytical methods for total Hg and MeHg in sediment and seawater along with supporting ancillary data are provided in *SI Appendix, Supplemental Analytical Methods Summary*. Hg isotope ratios in standard solutions were calculated daily, and the relative standard deviation remained below 2%. The limit of detection for $Me^{199}Hg$ and $Me^{200}Hg$ was <6 fM for seawater (methylated $^{199}/^{200}Hg^{II}$ in excess of natural isotope ratios) and 0.04 $pmol{\cdot}g^{-1}$ for sediment (42); $Me^{200}Hg$ in deionized water was below detection.

We developed an empirically constrained mass budget for water and sediments in Lake Melville using field data collected there for June and September. Methods for calculating reservoirs of individual Hg species, interconversions, and exchange among the sediment, water, and atmosphere follow Sunderland et al. (32) and are described in *SI Appendix*, Tables S6–S9, including error bounds. Our mass budget considers MeHg inputs to the water column from external sources (rivers, tides, atmospheric deposition,

benthic sediment) and in situ production and losses through settling of suspended solids, tidal outflow, and demethylation. The concentration of $Me^{199}Hg$ at the end of the experiment was not significantly different from the initial spike. On average, we recovered 98% of the initial $Me^{199}Hg$ spike at the conclusion of the experiment and thus, based on the change in $Me^{199}Hg$, infer that demethylation accounts for a maximum of $2\%{\cdot}d^{-1}$. Photodecomposition of MeHg is based on the total photosynthetically active radiation (RAD) penetrating the water column and the rate constant as a function of RAD ($0.0025/2.43 \times$ RAD) from Black et al. (43).

For annually averaged values, we consider the influence of ice cover/melt on evasion, seasonal variability in methylation caused by bacterial activity, and the pulse of Hg inputs associated with spring freshet. Full ice cover is generally present in Lake Melville between November and April. We assume evasion is negligible during these months because ice is thought to be a barrier for diffusing elemental Hg (Hg^0). Spring freshet occurs in late May–June and is associated with a large pulse of Hg inputs that we assume is 1 mo in duration based on peak river flow (13). Water-column methylation of Hg^{II} in marine systems is related to heterotrophic bacterial activity (7), and we thus assume that during ice-covered periods MeHg production is also minimal. We use the mean of measured methylation rates from Lake Melville, Goose Bay, and Groswater Bay (*SI Appendix*, Table S9) from the upper 10 m of the water column in June to calculate methylation occurring throughout the spring/summer period (May–June) and for the entire water column. We assume negligible water-column methylation for all other seasons in the annual budget. Extrapolation of the methylation rate for upper waters to the entire water column does not substantially change the annual budget, because 80% of the inorganic Hg in the system (160 mol) is contained in the stratified surface layer of the estuary (upper 15 m) because of elevated riverine inputs. Annual MeHg production (38 mol) thus increases by only 5% when bottom waters of the estuary are included.

ACKNOWLEDGMENTS. We thank the captains and crews of the MVs *What's Happening* and *Nuliajuk*; M. Biasutti-Brown, R. Laing, Z. Z. Kuzyk, C. Kamula, and V. Ortiz for field and laboratory support; and T. Sheldon (of the Nunatsiavut Government), T. Bell (Memorial University), and H. Amos and A. Pearson (Harvard University) for discussions and review of this work. This work was supported by the Nunatsiavut Government, National Science Foundation Grants OCE 1260464 and 1130549, ArcticNet Inc., and Tides Canada Oak Arctic Marine Fund Program.

1. Lavoie RA, Jardine TD, Chumchal MM, Kidd KA, Campbell LM (2013) Biomagnification of mercury in aquatic food webs: A worldwide meta-analysis. *Environ Sci Technol* 47(23):13385–13394.
2. Dewailly E, et al. (2001) Exposure of the Inuit population of Nunavik (Arctic Quebec) to lead and mercury. *Arch Environ Health* 56(4):350–357.
3. Stern GA, et al. (2012) How does climate change influence Arctic mercury? *Sci Total Environ* 414:22–42.
4. Hall BD, et al. (2005) Impacts of reservoir creation on the biogeochemical cycling of methyl mercury and total mercury in boreal upland forests. *Ecosystems (N Y)* 8(3): 248–266.
5. Benoit JM, Gilmour CC, Heyes A, Mason R, Miller C (2003) Geochemical and biological controls over methylmercury production and degradation in aquatic ecosystems. *ACS Symp* 835:1–33.
6. Compeau GC, Bartha R (1985) Sulfate-reducing bacteria: Principal methylators of mercury in anoxic estuarine sediment. *Appl Environ Microbiol* 50(2):498–502.
7. Sunderland EM, Krabbenhoft DP, Moreau JW, Strode SA, Landing WM (2009) Mercury sources, distribution, and bioavailability in the North Pacific Ocean: Insights from data and models. *Global Biogeochemical Cycles* 23(2):1–14.
8. Cossa D, et al. (2011) Mercury in the Southern Ocean. *Geochim Cosmochim Acta* 75(14):4037–4052.
9. Heimbürger L-E, et al. (2010) Methyl mercury distributions in relation to the presence of nano- and picophytoplankton in an oceanic water column (Ligurian Sea, Northwestern Mediterranean). *Geochim Cosmochim Acta* 74(19):5549–5559.
10. Wang F, Macdonald RW, Armstrong DA, Stern GA (2012) Total and methylated mercury in the Beaufort Sea: The role of local and recent organic remineralization. *Environ Sci Technol* 46(21):11821–11828.
11. Lehnherr I, St. Louis VL, Hintelmann H, Kirk JL (2011) Methylation of inorganic mercury in polar marine waters. *Nat Geosci* 4(5):298–302.
12. Heimbürger LE, et al. (2015) Shallow methylmercury production in the marginal sea ice zone of the central Arctic Ocean. *Sci Rep* 5:10318.
13. Bobbitt J, Akenhead SA (1982) Influence of controlled discharge from the Churchill River on the oceanography of Groswater Bay, Labrador. *Canadian Technical Report of Fisheries and Aquatic Sciences, No. 1097; Technical Report (Canada. Department of Fisheries and Oceans. Newfoundland Region. Research and Resource Services)*, (St. John's, Newfoundland, Canada).
14. St Louis VL, et al. (2004) The rise and fall of mercury methylation in an experimental reservoir. *Environ Sci Technol* 38(5):1348–1358.
15. Rolfhus KR, Hurley JP, Bodaly RA, Perrine G (2015) Production and retention of methylmercury in inundated boreal forest soils. *Environ Sci Technol* 49(6):3482–3489.
16. Sharif A, et al. (2014) Fate of mercury species in the coastal plume of the Adour River estuary (Bay of Biscay, SW France). *Sci Total Environ* 496:701–713.
17. Ortiz VL, Mason RP, Ward EJ (2015) An examination of the factors influencing mercury and methylmercury particulate distributions, methylation and demethylation rates in laboratory-generated marine snow. *Mar Chem*, in press.
18. Sholkovitz ER (1976) Flocculation of dissolved organic and inorganic matter during the mixing of river water and seawater. *Geochim Cosmochim Acta* 40(1966):831–845.
19. Long RA, Azam F (2001) Antagonistic interactions among marine pelagic bacteria. *Appl Environ Microbiol* 67(11):4975–4983.
20. Wikner J, Cuadros R, Jansson M (1999) Differences in consumption of allochthonous DOC under limnic and estuarine conditions in a watershed. *Aquat Microb Ecol* 17:289–299.
21. Hammerschmidt CR, Finiguerra MB, Weller RL, Fitzgerald WF (2013) Methylmercury accumulation in plankton on the continental margin of the northwest Atlantic Ocean. *Environ Sci Technol* 47(8):3671–3677.
22. Pućko M, et al. (2014) Transformation of mercury at the bottom of the Arctic food web: An overlooked puzzle in the mercury exposure narrative. *Environ Sci Technol* 48(13):7280–7288.
23. Sullivan JM, et al. (2010) Layered organization in the coastal ocean: An introduction to planktonic thin layers and the LOCO project. *Cont Shelf Res* 30(1):1–6.
24. Berdalet E, et al. (2014) Understanding harmful algae in stratified systems: Review of progress and future directions. *Deep Sea Res Part II Top Stud Oceanogr* 101:4–20.
25. Alldredge AL, et al. (2002) Occurrence and mechanisms of formation of a dramatic thin layer of marine snow in a shallow Pacific fjord. *Mar Ecol Prog Ser* 233:1–12.
26. Donaghay P, Rines H, Sieburth J (1992) Simultaneous sampling of fine scale biological, chemical, and physical structure in stratified waters. *Ergebnisse der Limnol ERLIA* 6(36):97–108.
27. Zemmelink HJ, et al. (2008) Stratification and the distribution of phytoplankton, nutrients, inorganic carbon, and sulfur in the surface waters of Weddell Sea leads. *Deep Res Part II Top Stud Oceanogr* 55(8-9):988–999.
28. Benoit-Bird KJ, Moline MA, Waluk CM, Robbins IC (2010) Integrated measurements of acoustical and optical thin layers I: Vertical scales of association. *Cont Shelf Res* 30(1): 17–28.
29. Falk-Petersen S, et al. (2008) Vertical migration in high Arctic waters during autumn 2004. *Deep Res Part II Top Stud Oceanogr* 55:2275–2284.
30. Arendt KE, Nielsen TG, Rysgaard S, Tönnesson K (2010) Differences in plankton community structure along the Godthåbsfjord, from the Greenland Ice Sheet to offshore waters. *Mar Ecol Prog Ser* 401:49–62.
31. Blachowiak-Samolyk K, Kwasniewski S, Dmoch K, Hop H, Falk-Petersen S (2007) Trophic structure of zooplankton in the Fram Strait in spring and autumn 2003. *Deep Res Part II Top Stud Oceanogr* 54(23-26):2716–2728.
32. Sunderland EM, et al. (2010) Response of a macrotidal estuary to changes in anthropogenic mercury loading between 1850 and 2000. *Environ Sci Technol* 44(5): 1698–1704.
33. Nalcor Energy (2009) *Lower Churchill Hydroelectric Generation Project: Environmental Impact Statement; Executive Summary* (Nalcor Energy, St. Johns, Newfoundland, Canada), p 63.
34. Hollweg TA, Gilmour CC, Mason RP (2010) Mercury and methylmercury cycling in sediments of the mid-Atlantic continental shelf and slope. *Limnol Oceanogr* 55(6): 2703–2722.
35. Jonsson S, et al. (2014) Differentiated availability of geochemical mercury pools controls methylmercury levels in estuarine sediment and biota. *Nat Commun* 5:4624.
36. Wassmann P (2011) Arctic marine ecosystems in an era of rapid climate change. *Prog Oceanogr* 90(1-4):1–17.
37. Gill G, Fitzgerald WF (1985) Mercury sampling of open ocean waters at the picomolar level. *Deep-Sea Res A, Oceanogr Res Pap* 32(3):287–297.
38. Hintelmann H, Ogrinc N (2003) Determination of stable mercury isotopes by ICP/MS and their application in environmental studies. *ACS Symp Ser* 835:321–338.
39. Gilmour C, Riedel G (1995) Measurement of Hg methylation in sediments using high specific-activity 203 Hg and ambient incubation. *Water Air Soil Pollut* 80(1):747–756.
40. Schartup AT, Mason RP, Balcom PH, Hollweg TA, Chen CY (2013) Methylmercury production in estuarine sediments: Role of organic matter. *Environ Sci Technol* 47(2): 695–700.
41. Hammerschmidt CR, Fitzgerald WF (2008) Sediment–water exchange of methylmercury determined from shipboard benthic flux chambers. *Mar Chem* 109(1-2):86–97.
42. Hintelmann H, Evans RD (1997) Application of stable isotopes in environmental tracer studies - Measurement of monomethylmercury ($CH_3\ Hg^+$) by isotope dilution ICP-MS and detection of species transformation. *Fresenius J Anal Chem* 358(3):378–385.
43. Black FJ, Poulin BA, Flegal AR (2012) Factors controlling the abiotic photo-degradation of monomethylmercury in surface waters. *Geochim Cosmochim Acta* 84:492–507.